Original Article

PROGRESS in MEDICAL PHYSICS 27(4), Dec. 2016
https://doi.org/10.14316/pmp.2016.27.4.236
pISSN 2508-4445, eISSN 2508-4453

Conceptual Study of Brain Dedicated PET Improving Sensitivity

Han-Back Shin*, Yong Choi†, Yoonsuk Huh†, Jin Ho Jung†, Tae Suk Suh*

*Department of Biomedical Engineering and Research Institute of Biomedical Engineering, College of Medicine, The Catholic University of Korea, †Department of Electronic Engineering, Sogang University, Seoul, Korea

The purpose of this study is to propose a novel high sensitivity neuro-PET design. The improvement of sensitivity in neuro-PET is important because it can reduce scan time and/or radiation dose. In this study, we proposed a novel PET detector design that combined conical shape detector with cylindrical one to obtain high sensitivity. The sensitivity as a function of the oblique angle and the ratio of the conical to cylindrical portion was estimated to optimize the design of brain PET using Monte Carlo simulation tool, GATE. An axial sensitivity and misplacement rate by penetration of γ rays were also estimated to evaluate the performance of the proposed PET. The sensitivity was improved by 36% at the center of axial FOV. This value was similar to the calculated value. The misplacement rate of conical shaped PET was about 5% higher than the conventional PET. The results of this study demonstrated the conical detector proposed in this study could provide subsequent improvement in sensitivity which could allow to design high sensitivity PET for brain imaging.

Key Words: Neuro-PET, GATE, High sensitivity

Introduction

A dedicated brain scanner can provide high spatial resolution images for diagnosis of neuro disease such as brain cancer and Alzheimer's disease, while also providing a count rate capability sufficient to study physiologic effects with fast temporal dynamics.[1] Dedicated brain PET scanners with a small detector ring diameter provide large solid-angle coverage of the human head, leading to higher sensitivity per unit detector volume compared to a multipurpose whole-body PET scanner.[2,3] The increased sensitivity achieved by such scanners comes with decreased noncolinearity degradation of the spatial resolution but with greater parallax and solid-angle effects.[1,4,5] Small ring design makes dedicated brain PET desirable for use in many imaging procedures. However, there is a potential drawback of such a small ring design-namely, increased scatter and random coincidences, particularly in 3-dimensional (3D) imaging.

The improvement of sensitivity in a neoro-PET is crucial because it can reduce the scan time and/or the radiation dose. In this study, we proposed a novel PET detector design that combined conical shape detector with cylindrical one to obtain high sensitivity as illustrated in Fig. 1. The NECR as a function of the oblique angle and the ratio of conical to cylindrical portion was estimated to optimize the design of proposed PET using Monte Carlo simulation tool, GATE.[6,7] An axial sensitivity and misplacement rate by penetration of γ rays were also estimated to evaluate the performance of the brain dedicated PET design.

This work was supported by the Joint Research Program funded by The Catholic University of Korea-Sogang University (2016).
Yoonsuk Huh is now with the Advanced R&D team, Health and Medical Equipment Business, Samsung Electronics Co., Ltd., Gyeonggi-do, Korea.
Received 16 December 2016, Revised 23 December 2016, Accepted 23 December 2016
Correspondence: Tae Suk Suh (suhsanta@catholic.ac.kr)
Tel: 82-2-2258-7232, Fax: 82-2-2258-7506
Co-correspondence: Yong Choi (ychoi@sogang.ac.kr)
Tel: 82-2-705-8910, Fax: 82-2-713-2652

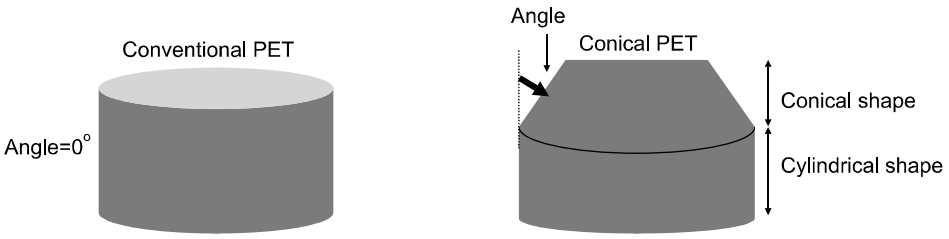

Fig. 1. Diagram of the Conventional PET (left) and Conical PET (right). Conventional PET was consisted of cylindrical shape and conical PET was consisted of cylindrical and conical shape having angle.

Table 1. Configurations of conventional PET and conical PET.

	Conventional PET	Conical PET
Diameter (D)	390 mm	250 mm < D < 390 mm*
Axial length (AL)	246 mm	236 mm < AL < 254 mm depending on the angle and ratio
Number of crystals per ring (NOC)	363	130 < NOC < 363 depending on the angle and ratio
Time window, energy window	10 ns, 410 ~ 613 keV	
Crystal size (LYSO)	3×3×20 mm^3	
Detector area	2,384 cm^2	

Materials and Methods

1. Configurations of conventional PET and proposed design PET

Conventional PET and conical PET were simulated using Monte Carlo simulation tool, GATE.[6,7] Fig. 1 shows the diagram of simulated geometry of conventional PET and conical PET combing conical shape detector with cylindrical one. The energy window range was set to 20% of the 511 keV photopeak.[4,8] The system configurations were summarized in Table 1.

2. Determination of the angle and ratio

The effects of the angle and ratio on the true, scatter, random coincidence count and noise equivalent count rate (NECR) of conical PET were also investigated using GATE.[6,7] The angle of conical PET was varied from 20° to 50° with 10° intervals, while the ratio between the cylindrical and conical portion was fixed at 5:5. After then, sensitivity of conical PET with optimal angle as a function of ratio were also estimated. Additionally, these results were compared to that of the conventional PET. NECR was defined by the following equation.

$$NECR = \frac{T^2}{T + S + 2R} \quad \text{(Eq. 1)}$$

where T, S and R are the true, scatter, random count rate, respectively.

3. Axial sensitivity

The axial sensitivity was estimated by moving ^{18}F Point source with 25 mm increments in the axial direction with both conventional and conical PET.

The list-mode data of the conical PET and conventional PET were used to estimate the axial sensitivity.

Geometric efficiency is influenced by axial length and diameter. The conical PET has a greater solid angle then the conventional PET. To validate the simulation result, the geometric efficiency was analytically calculated as follows[5]:

$$\text{Geometric efficiency} = \frac{A}{D} \quad \text{(Eq. 2)}$$

where A is the axial length and D is the ring diameter.

4. Misplacement rate

Misplacement rate might be increased in the conical PET because conical PET increases the fraction of γ rays obliquely incident to the detector surface. To estimate the misplacement rate caused by penetration of γ rays, the detector position of incident γ rays was compared with the detector position of coincidence events.[6,7,9-11] If the detector position of incident γ rays was not corresponded with the position of co-

incidence events, it was considered as the misplacement event caused by penetration of γ rays. Misplacement rate of conical PET and conventional PET as a function of axial detector position was estimated using the point source at the center of axial FOV.

5. Imaging capability

To evaluate the imaging capability of the conical PET, hot-rod phantoms filled with 100 kBq ^{18}F was used and located in the center of FOV. No attenuation, random or scatter correction were applied in this imaging studies. PET images were reconstructed by 2D filtered backprojection (2D FBP) using a Hanning filter with a cutoff at the Nyquist frequency.[12)]

Results

1. Determination of the angle and the ratio

Table 2 and 3 shows the true, scatter, random coincidence and NECR of the conventional PET and conical PET as a function angle and ratio.

Table 2. The noise equivalent count rate (NECR) of conventional PET and conical PET according to the angle of conical PET.

		Axial length (mm)	Improvement rate (%) (Conical/Conventional)			
			True	Scatter	Random	NECR
Conventional PET		246	100	100	100	100
Conical PET	20°	254	114	113	147	115
	30°	251	134	130	165	136
	40°	245	143	139	138	145
	50°	238	161	151	152	165

Table 3. The noise equivalent count rate (NECR) of conventional PET and Conical PET as a function of the ratio of conical portion.

		Axial length (mm)	Improvement rate (%) (Conical/Conventional)			
			True	Scatter	Random	NECR
Conventional PET		246	100	100	100	100
Conical PET	4:6	250	159	145	225	165
	5:5	245	143	139	138	145
	6:4	236	126	123	96	128

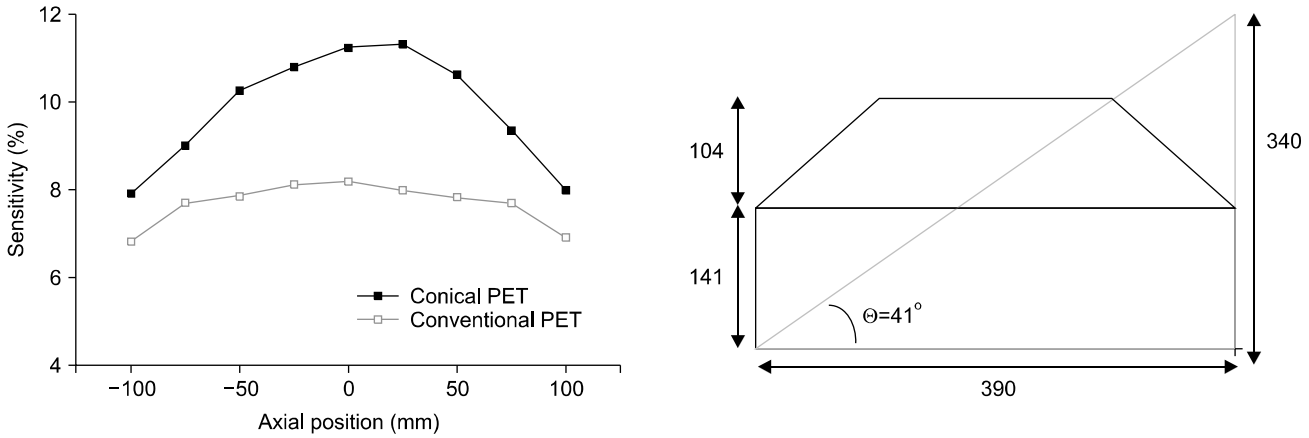

Fig. 2. Axial sensitivity of conical PET and conventional PET (left). Diameter (390 mm) and axial length (340 mm) of conical PET based on the analytical model (right).

As illustrated in Table 2, 50° was proper to obtain high NECR value. On the other hand, the axial length of 50° was shorter than the conventional PET. Then, considering the axial length and sensitivity, 40° was selected for evaluation regarding the angle variance between two portions.

Considering the sensitivity and NECR, 4 to 6 ratio was the best option as shown in Table 3. However, the 5:5 was selected because the diameter of 4:6 was smaller than the maximum head width of adult male (223 mm).

Table 4. Misplacement rate of conical PET and conventional PET.

	Misplacement rate
Conical PET	65.2%
Conventional PET	59.6%

2. Axial sensitivity

The axial sensitivity was estimated to evaluate the performance of the conical PET design using the optimized parameters of the angle (40°) and the ratio (5:5).

The sensitivity of the conical PET compared with the conventional PET was improved 36% at the center of axial FOV as shown in Fig. 2. This is due to the greater geometric efficiency of the conical PET. The expected increase in sensitivity is 38% calculated by the Fig. 2 (right) and Eq. 2, which was in good accordance with the simulated value.

3. Misplacement rate

As seen in Table 4 the misplacement rate of conical PET

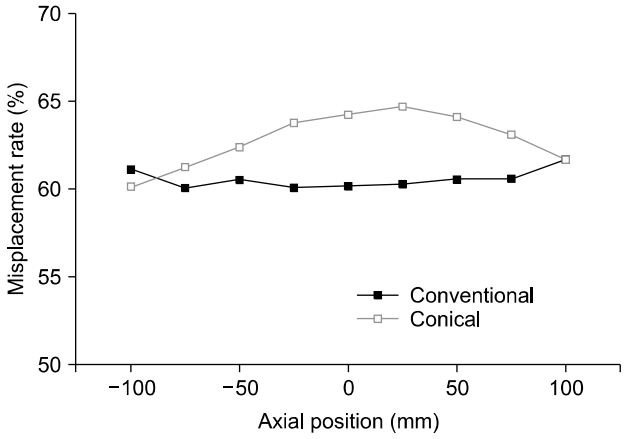

Fig. 3. The misplacement rate of conventional PET and conical PET as a function of axial position.

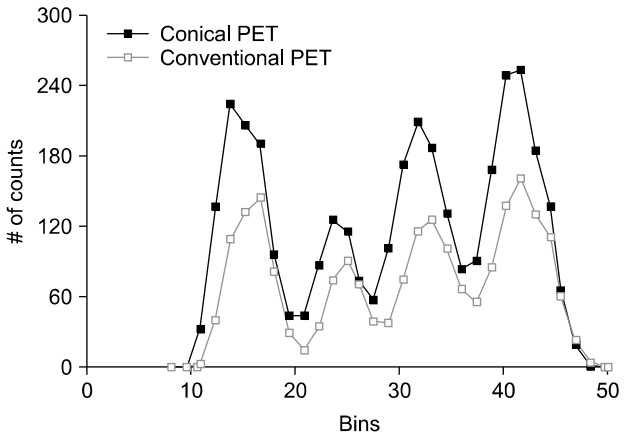

Fig. 5. Image profile drawn through the 3.5 mm size of hot-rod phantom.

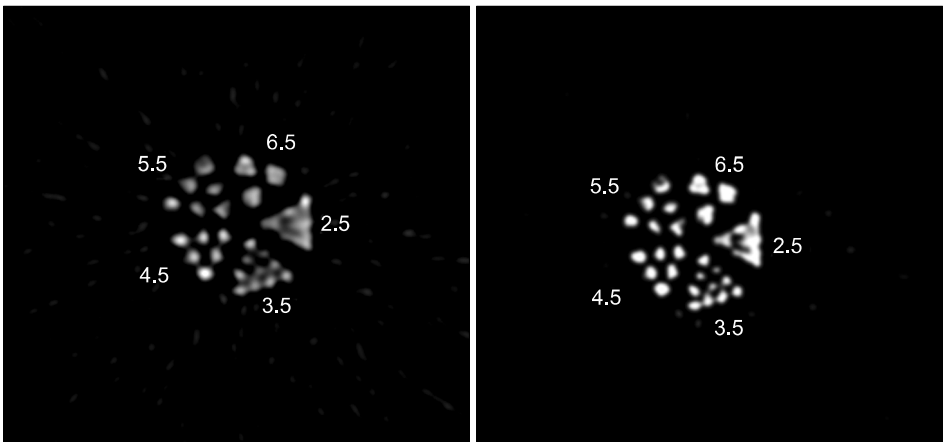

Fig. 4. Tomography images of hot-rod phantom for conventional PET (left) and conical PET (right).

was about 5% higher than the conventional PET. And Fig. 3 shows the misplacement rate according to the axial position of PET detector.

4. Imaging capability

As shown in Fig. 4, the rods down to a diameter of 3.5 mm were resolve in the tomographic images of the hot-rod phantom. Fig. 5 shows the line profiles drawn through the 3.5 mm size of hot-rod phantom. It shows higher signal-to-noise ratio of the image acquired with conical PET than that of the conventional PET.

Discussion and Conclusion

In this study, the effects of angle and ratio on the sensitivity of conical PET were characterized and the optimal angle and ratio for a conical PET were derived.

Conical PET proposed in this study has the several advantages. First of all, the result of sensitivity demonstrated the conical PET could provide improvement in sensitivity which could allow to design high sensitivity PET for brain imaging which allows to reduce the scan time and/or radiation dose. Secondly, imaging quality of the conical PET might be improved in comparison with the conventional PET because the NECR of conical PET compared with the conventional PET was increased. Lastly, even though conventional PET and conical PET had the equal detector area, conical PET has high sensitivity without any additional cost.

Analytically predicted sensitivity improvement of conical PET was in good accordance with the simulation results at the center of FOV as illustrated in Fig. 2.

Further study will be performed to estimate the misplacement of along with the axial position and the position correction algorithm will be developed for the 3D image reconstruction.

References

1. J. S. Karp, S. Surti, E. Daube-Witherspoon, et al: Performance of a Brain PET Camera Based on Anger-Logic Gadolinium Oxyorthosilicate Detectors. J Nucl Med 44:1340-1349 (2003)
2. E. J. Hoffman, M. E Phelps, S. C Huang, et al: Performance evaluation of a positron tomograph designed for brain imaing. J Nucl Med 24:245-257 (1983)
3. C. Knoess, S. Siegel, et al: Performance evaluation of the micro PET R4 PET scanner for rodents. Eur J Nucl Med Mol Imaging 30:737-747 (2003)
4. S. Jan, G. Santin, D. Strul, et al: GATE: a simulation toolkit for PET and SPECT. Phys. Med. Biol 49:4543 (2004)
5. Y. Shao, S. R. Cherry, S. Siegel, et al: A study of inter-crystal scatter in small scintillator arrays designed for high resoultion PET imaging, IEEE Trans. Nuc. Sci 43:1938-1944 (1996)
6. I. Buvat, D. Lazaro: Monte Carlo simulations in emission tomography and GATE: an overview. Nucl. Instr. Meth. Phys. Res 569:323-329 (2006)
7. S. R. Cherry, J. A. Sorenson, M. E. Phelps: Physics in Nuclear Medicine 3rd ed. Philadelphia:Saunders (2004)
8. D.L. Bailey, S. R. Meikle: A convolution-subtraction scatter correction method for 3D PET. Phys Med Biol 39:411 (1994)
9. S. Moehrs, A. Del Guerra, D. J. Herbert, M. A. Mandelkern: A detector head design for small-animal PET with silicon photomultipliers (SiPM). Phys Med Biol 51:1113-1127 (2006)
10. A. Bartoli, N. Belcari, A. Del Guerra, S. Fabbri: Simultaneous PET/SPECT imaging with the small animal scanner YAP-(S) PET. IEEE Nucl Sci Symp Conf Rec 5:3408-13 (2007)
11. R. Yao, J. F. Beaudoin, X. Deng, J. Cadorette, et al: Imaging performance of a PET/SPECT dual modality animal system. IEEE Nucl Sci Symp Conf Rec 2418-21 (2011)
12. Y. C. Tai, A. Ruangma, D. Rowland, et al: Performance evaluation of the microPET focus: a third-generation microPET scanner dedicated to animal imaing. J Nucl Med 46:455-463 (2005)